# Transient Zitterbewegung of charge carriers in mono- and bilayer graphene, and carbon nanotubes

Tomasz M. Rusin[1,*] and Wlodek Zawadzki[2]
[1]*PTK Centertel Sp. z o.o., ulica Skierniewicka 10A, 01-230 Warsaw, Poland*
[2]*Institute of Physics, Polish Academy of Sciences, Al. Lotników 32/46, 02-688 Warsaw, Poland*
(Received 24 April 2007; published 27 November 2007)

Observable effects due to trembling motion [Zitterbewegung (ZB)] of charge carriers in bilayer graphene, monolayer graphene, and carbon nanotubes are calculated. It is shown that, when the charge carriers are prepared in the form of Gaussian wave packets, the ZB has a transient character with the decay time of femtoseconds in graphene and picoseconds in nanotubes. Analytical results for bilayer graphene allow us to investigate phenomena which accompany the trembling motion. In particular, it is shown that the transient character of ZB in graphene is due to the fact that wave subpackets related to positive and negative electron energies move in opposite directions, so their overlap diminishes with time. This behavior is analogous to that of the wave packets representing relativistic electrons in a vacuum.

DOI: 10.1103/PhysRevB.76.195439 PACS number(s): 73.22.−f, 03.65.Pm, 73.63.Fg, 78.67.Ch

## I. INTRODUCTION

The trembling motion [Zitterbewegung (ZB)], first devised by Schrödinger for free relativistic electrons in a vacuum,[1] has become in the last two years a subject of great theoretical interest as it has turned out that this phenomenon should occur in many situations in semiconductors.[2–10] Whenever one deals with two or more energy branches, an interference of the corresponding upper and lower energy states results in the trembling motion even in the absence of external fields. Due to a formal similarity between two interacting bands in a solid and the Dirac equation for relativistic electron in a vacuum one can use methods developed in the relativistic quantum mechanics for nonrelativistic electrons in solids.[11,12] Most of the ZB studies for semiconductors took as a starting point plane electron waves. Some authors treated the case of Gaussian wave packets.[5,7,13,14] Katsnelson,[6] Cserti and David,[8] Trauzettel *et al.*[10] studied theoretically ZB in monolayer and bilayer graphene using the plane wave representation. On the other hand, Lock[14] in his important paper observed that "such a wave is not localized and it seems to be of a limited practicality to speak of rapid fluctuations in the average position of a wave of infinite extent." Using the Dirac equation Lock showed that, when an electron is represented by a wave packet, the ZB oscillations do not remain undamped but become transient. In particular, the disappearance of oscillations at sufficiently large times is guaranteed by the Riemann-Lebesgue theorem as long as the wave packet is a smoothly varying function. Since the ZB is by its nature not a stationary state but a dynamical phenomenon, it is natural to study it with the use of wave packets. These have become a practical instrument when femtosecond pulse technology emerged (see Ref. 15).

In the following, we study theoretically the Zitterbewegung of mobile charge carriers in three modern materials: bilayer graphene, monolayer graphene, and carbon nanotubes. We have three objectives in mind. First, we obtain analytical results for the ZB of Gaussian wave packets which allows us to study not only the trembling motion itself but also effects that accompany this phenomenon. Second, we describe the transient character of ZB in solids, testing on specific examples the general predictions of Ref. 14. Third, we look for observable phenomena and select both systems and parameters which appear most promising for experiments. We first present our analytical results for bilayer graphene and then quote some predictions for observable quantities in monolayer graphene and carbon nanotubes.

## II. BILAYER GRAPHENE

Two-dimensional Hamiltonian for bilayer graphene is well approximated by[16]

$$\hat{H}_B = -\frac{1}{2m^*}\begin{pmatrix} 0 & (\hat{p}_x - i\hat{p}_y)^2 \\ (\hat{p}_x + i\hat{p}_y)^2 & 0 \end{pmatrix}, \tag{1}$$

where $m^*=0.054m_0$. Form (1) is valid for energies $2<\mathcal{E}<100$ meV in the conduction band. The energy spectrum is $\mathcal{E}=\pm E$, where $E=\hbar^2k^2/2m^*$, i.e., there is no energy gap between the conduction and valence bands. The position operator in the Heisenberg picture is a $2\times 2$ matrix $\hat{x}(t)=\exp(i\hat{H}_Bt/\hbar)\hat{x}\exp(-i\hat{H}_Bt/\hbar)$. We calculate

$$x_{11}(t) = x(0) + \frac{k_y}{k^2}\left[1 - \cos\left(\frac{\hbar k^2 t}{m^*}\right)\right], \tag{2}$$

where $k^2=k_x^2+k_y^2$. The third term represents the Zitterbewegung with the frequency $\hbar\omega_Z=2\hbar^2k^2/2m^*$, corresponding to the energy difference between the upper and lower energy branches for a given value of $k$.

We want to calculate the ZB of a charge carrier represented by a two-dimensional wave packet,

$$\psi(\boldsymbol{r},0) = \frac{1}{2\pi}\frac{d}{\sqrt{\pi}}\int d^2\boldsymbol{k}e^{-(1/2)d^2k_x^2-(1/2)d^2(k_y-k_{0y})^2}e^{i\boldsymbol{kr}}\begin{pmatrix}1\\0\end{pmatrix}. \tag{3}$$

The packet is centered at $\boldsymbol{k}_0=(0,k_{0y})$ and is characterized by a width $d$. The unit vector (1,0) is a convenient choice, selecting the 11 component of $\hat{x}(t)$ [see Eq. (2)]. An average of

 ©2007 The American Physical Society

$\hat{x}_{11}(t)$ is a two-dimensional integral which we calculate analytically,

$$\bar{x}(t) = \langle \psi(\boldsymbol{r}) | \hat{x}(t) | \psi(\boldsymbol{r}) \rangle = \bar{x}_c + \bar{x}_Z(t), \tag{4}$$

where $\bar{x}_c = (1/k_{0y})[1 - \exp(-d^2 k_{0y}^2)]$, and

$$\bar{x}_Z(t) = \frac{1}{k_{0y}} \left[ \exp\left( -\frac{\delta^4 d^2 k_{0y}^2}{d^4 + \delta^4} \right) \cos\left( \frac{\delta^2 d^4 k_{0y}^2}{d^4 + \delta^4} \right) - \exp(-d^2 k_{0y}^2) \right], \tag{5}$$

in which $\delta = \sqrt{\hbar t / m^*}$ contains the time dependence. We enumerate the main features of ZB following from Eqs. (4) and (5). First, in order to have the ZB in the $x$ direction, one needs an initial transverse momentum $\hbar k_{0y}$. Second, the ZB frequency depends only weakly on the packet width: $\omega_Z = (\hbar k_{0y}^2 / m^*)[d^4/(d^4 + \delta^4)]$, while its amplitude is strongly dependent on the width $d$. Third, the ZB has a transient character, as it is attenuated by the exponential term. For small $t$, the amplitude of $\bar{x}_Z(t)$ diminishes as $\exp(-\Gamma_Z^2 t^2)$, with

$$\Gamma_Z = \frac{\hbar k_{0y}}{m^* d}. \tag{6}$$

Fourth, as $t$ (or $\delta$) increases, the cosine term tends to unity and the first term in Eq. (5) cancels out with the second term, which illustrates the Riemann-Lebesgue theorem (see Ref. 14). After the oscillations disappear, the charge carrier is displaced by the amount $\bar{x}_c$, which is a "remnant" of ZB. Fifth, for very wide packets ($d \to \infty$), the exponent in Eq. (5) tends to unity, the oscillatory term is $\cos(\delta^2 k_{0y}^2)$, and the last term vanishes. In this limit, we recover undamped ZB oscillations.

Next, we consider observable quantities related to the ZB, beginning by the current. The latter is given by the velocity multiplied by charge. The velocity is simply $\bar{v}_x = \partial \bar{x}_Z / \partial t$, where $\bar{x}_Z$ is given by Eq. (5). The calculated current is plotted in Fig. 1(b), its oscillations are a direct manifestation of ZB. The Zitterbewegung is also accompanied by a time dependence of upper and lower components of the wave function. To characterize this evolution, we define probability densities for the upper and lower components,

$$P_\pm(t) = \left\langle \psi(\boldsymbol{r},t) \left| \frac{1 \pm \hat{\beta}}{2} \right| \psi(\boldsymbol{r},t) \right\rangle, \tag{7}$$

where

$$\hat{\beta} = \begin{pmatrix} 1 & 0 \\ 0 & -1 \end{pmatrix},$$

and the time-dependent wave function is $\psi(\boldsymbol{r},t) = \exp(-i\hat{H}_B t/\hbar)\psi(\boldsymbol{r},0)$. We have

$$\psi(\boldsymbol{r},t) = \frac{1}{2\pi} \frac{d}{\sqrt{\pi}} \int d^2\boldsymbol{k} e^{-(1/2)d^2 k_x^2 - (1/2)d^2 (k_y - k_{0y})^2} \times e^{i\boldsymbol{k}\boldsymbol{r}} \begin{pmatrix} \cos(\hbar k^2 t/2m) \\ i(k_+/k)^2 \sin(\hbar k^2 t/2m) \end{pmatrix}, \tag{8}$$

where $k_+ = k_x + ik_y$. For $t=0$, Eq. (8) reduces to Eq. (3). The calculated probability densities are

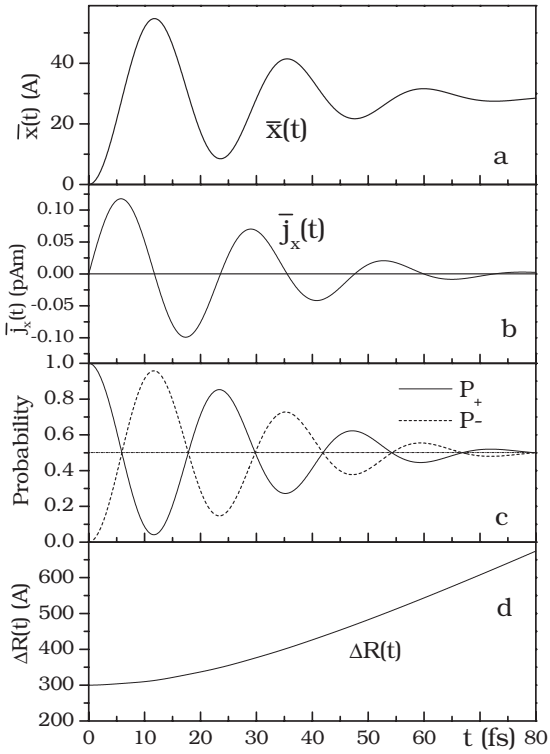


FIG. 1. Zitterbewegung of a charge carrier in bilayer graphene versus time, calculated for a Gaussian wave packet width $d = 300$ Å and $k_{0y} = 3.5 \times 10^8$ m$^{-1}$: (a) displacement, (b) electric current, (c) probability densities for upper and lower components of the wave function, and (d) dispersion $\Delta R(t)$. The decay time is $\Gamma_Z^{-1} = 40$ fs [see Eq. (6)].

$$P_\pm(t) = \frac{1}{2} \pm \frac{1}{2} \frac{d^2}{s^4} \exp\left( -\frac{\delta^4 d^2 k_{0y}^2}{s^4} \right) \left[ d^2 \cos\left( \frac{\delta^2 d^4 k_{0y}^2}{s^4} \right) - \delta^2 \sin\left( \frac{\delta^2 d^4 k_{0y}^2}{s^4} \right) \right], \tag{9}$$

where $s^4 = d^4 + \delta^4$. The time dependence of $P_\pm(t)$ is illustrated in Fig. 1(c). Clearly, there must be $P_+(t) + P_-(t) = 1$ at any time, but it is seen that the probability density "flows" back and forth between the two components. It is clear that the oscillating probability is directly related to ZB. In bilayer graphene, the upper and lower components are associated with the A1 and B2 atoms, respectively (here 1-2 stand for top and bottom and A-B stands for the inequivalent atom sites of the honeycomb lattice[17]). For sufficiently long times, there is $P_\pm = 1/2$, so that the final probability is equally distributed. For a very wide packet ($d \to \infty$), we have $P_\pm = (1/2)[1 \pm \cos^2(\delta^2 k_{0y}^2)]$, which indicates that the probability oscillates without attenuation. For $k_{0y} = 0$, there is $P_\pm = (1/2)[1 \pm d^4/s^4]$, i.e., there are no oscillations and the initial probability (1,0) simply decays into $(1/2, 1/2)$.

The above phenomenon can be considered from the point of view of the entropy: $S = -P_+ \log_2 P_+ - P_- \log_2 P_-$. At the beginning the entropy is zero and at the end (when the probability is equally distributed between the two components)

the entropy is $\log_2 2$. However, the entropy increases in the oscillatory fashion (see Ref. 18).

The transient character of ZB is accompanied by a temporal spreading of the wave packet. In fact, the question arises whether the attenuation of ZB is not simply *caused* by the spreading of the packet. To study this question, we calculate an explicit form of the wave function given by integral (8). The result is

$$\psi^{up}(\boldsymbol{r},t) = \frac{d}{\sqrt{\pi}s^4}\exp\left(-\frac{d^2\rho^2}{2s^4}\right)\exp\left(-\frac{\delta^4 d^2 k_{0y}^2}{2s^4}\right)\exp\left(\frac{iyd^4k_{0y}}{s^4}\right) \times\left[d^2\cos\left(\frac{\delta^2\rho_{k0}^2}{2s^4}\right)+\delta^2\sin\left(\frac{\delta^2\rho_{k0}^2}{2s^4}\right)\right], \tag{10}$$

$$\psi^{low}(\boldsymbol{r},t) = \frac{-id}{\sqrt{\pi}s^4}\exp\left(-\frac{d^2\rho^2}{2s^4}\right)\exp\left(-\frac{\delta^4 d^2 k_{0y}^2}{2s^4}\right)\exp\left(\frac{iyd^4k_{0y}}{s^4}\right) \times\left(\frac{x+iy+d^2k_{0y}}{\rho_{k0}}\right)^2\left[\left(\frac{2s^4}{\rho_{k0}^2}+d^2\right)\sin\left(\frac{\delta^2\rho_{k0}^2}{2s^4}\right) -\delta^2\cos\left(\frac{\delta^2\rho_{k0}^2}{2s^4}\right)\right], \tag{11}$$

where $\rho^2=x^2+y^2$ and $\rho_{k0}^2=x^2+(y-id^2k_{0y})^2$. It is seen that the packet, which was Gaussian at $t=0$ [see Eq. (3)], is *not* Gaussian at later times (see Discussion). The upper and lower components have the same decay time, oscillation period, etc. In order to characterize the spreading (or dispersion) of the packet we calculate its width $\Delta R(t)$ as a function of time,

$$[\Delta R(t)]^2 = \langle\psi(\boldsymbol{r},t)|\hat{\boldsymbol{r}}^2-\langle\hat{\boldsymbol{r}}\rangle^2|\psi(\boldsymbol{r},t)\rangle, \tag{12}$$

where $\psi(\boldsymbol{r},t)$ is the above two-component wave function and $\langle\hat{\boldsymbol{r}}\rangle=\langle\psi(\boldsymbol{r},t)|\hat{\boldsymbol{r}}|\psi(\boldsymbol{r},t)\rangle$. The calculated width $\Delta R$ is plotted versus time in Fig. 1(d). It is seen that during the initial 80 fs, the packet's width increases only twice compared to its initial value, while the ZB and the accompanying effects disappear almost completely during this time. We conclude that the spreading of the packet is *not* the main cause of the transient character of the ZB. In fact, also the spreading oscillates a little, but this effect is too small to be seen in Fig. 1(d).

It can be seen from the above equations that ZB characteristics depend on $(dk_{0y})$ argument. In consequence, if one diminishes (say) the packet width $d'=d/\lambda$ and increases correspondingly the initial wave vector $k'_{0y}=k_{0y}\lambda$, the quantities shown in Fig. 1 look roughly the same on the time scale $t'=t/\lambda^2$. Clearly, the packet width $d$ should be made larger than the interlayer distance and smaller than the mean free path of charge carriers in the material. If, for fixed $k_{0y}$, the width $d$ is much smaller than the value chosen for Fig. 1, the oscillation pattern contains fewer oscillations before complete attenuation. In contrast, for higher $d$ values, there occur more visible oscillations. The value of $k_{0y}$ was chosen to be within the validity range of the Hamiltonian [Eq. (1)] (see Ref. 16). If $k_{0y}$ goes above the validity range, the ZB still occurs, but it cannot be described with the use of analytical formulas.

It is well known that the phenomenon of ZB is due to an interference of wave functions corresponding to positive and negative eigenenergies of the initial Hamiltonian. Looking for physical reasons behind the transient character of ZB described above, we decompose the total wave function $\psi(\boldsymbol{r},t)$ into the positive $(p)$ and negative $(n)$ components $\psi^p(\boldsymbol{r},t)$ and $\psi^n(\boldsymbol{r},t)$. We have

$$|\psi(t)\rangle = e^{-i\hat{H}t/\hbar}|\psi(0)\rangle = e^{-iEt/\hbar}\langle p|\psi(0)\rangle|p\rangle + e^{iEt/\hbar}\langle n|\psi(0)\rangle|n\rangle, \tag{13}$$

where $|p\rangle$ and $|n\rangle$ are the eigenfunctions of the Hamiltonian [Eq. (1)] in $\boldsymbol{k}$ space corresponding to positive and negative energies, respectively. Further,

$$\langle\boldsymbol{k}|p\rangle = \frac{1}{\sqrt{2}}\begin{pmatrix}1\\ k_+^2/k^2\end{pmatrix}\delta(\boldsymbol{k}-\boldsymbol{k}'), \tag{14}$$

$$\langle\boldsymbol{k}|n\rangle = \frac{1}{\sqrt{2}}\begin{pmatrix}1\\ -k_+^2/k^2\end{pmatrix}\delta(\boldsymbol{k}-\boldsymbol{k}'). \tag{15}$$

After some manipulations, we finally obtain

$$\psi^p(\boldsymbol{r},t) = \frac{1}{4\pi}\frac{d}{\sqrt{\pi}}\int d^2\boldsymbol{k}e^{-(1/2)d^2[k_x^2+(k_y-k_{0y})^2]}e^{i\boldsymbol{k}\boldsymbol{r}}e^{-iEt/\hbar}\begin{pmatrix}1\\ k_+^2/k^2\end{pmatrix}. \tag{16}$$

The function $\psi^n(\boldsymbol{r},t)$ is given by the identical expression with the changed signs in front of $E$ and $k_+^2/k^2$ terms. There is $\psi(\boldsymbol{r},t)=\psi^p(\boldsymbol{r},t)+\psi^n(\boldsymbol{r},t)$ and $\langle\psi^n|\psi^p\rangle=0$.

Now, we calculate the average values of $\bar{x}$ and $\bar{y}$ using the positive and negative components in the above sense. We have

$$\bar{x}(t) = \int(\psi^n+\psi^p)^\dagger x(\psi^n+\psi^p)d^2\boldsymbol{r}, \tag{17}$$

so that we deal with four integrals. A direct calculation gives

$$\int|\psi^p|^2xd^2\boldsymbol{r}+\int|\psi^n|^2xd^2\boldsymbol{r}=\bar{x}_c, \tag{18}$$

$$\int\psi^{n\dagger}x\psi^p d^2\boldsymbol{r}+\int\psi^{p\dagger}x\psi^n d^2\boldsymbol{r}=\bar{x}_Z(t), \tag{19}$$

where $\bar{x}_c$ and $\bar{x}_Z(t)$ have been defined in Eq. (4). Thus, the integrals involving only the positive and only the negative components give the constant shift due to ZB, while the mixed terms lead to the ZB oscillations. All terms together reconstruct result (4).

Next, we calculate the average value $\bar{y}$. There is no symmetry between $\bar{x}$ and $\bar{y}$ because the wave packet is centered around $k_x=0$ and $k_y=k_{0y}$. The average value $\bar{y}$ is again given by four integrals. However, now the mixed terms vanish since they contain odd integrands of $k_x$, while the integrals involving the positive and negative components alone give

$$\int |\psi^p|^2 y d^2\boldsymbol{r} = \frac{\hbar k_{0y}}{2m^*}t, \tag{20}$$

$$\int |\psi^n|^2 y d^2\boldsymbol{r} = -\frac{\hbar k_{0y}}{2m^*}t. \tag{21}$$

This means that the "positive" and "negative" subpackets move in the opposite directions with the same velocity $v=\hbar k_{0y}t/2m^*$. The relative velocity is $v^{rel}=\hbar k_{0y}t/m^*$. Each of these packets has the initial width $d$ and it (slowly) spreads in time. After the time $\Gamma_Z^{-1}=d/v^{rel}$, the distance between the two packets equals $d$, so the integrals [Eq. (18)] are small, resulting in the diminishing Zitterbewegung amplitude. This reasoning gives the decay constant $\Gamma_Z=\hbar k_{0y}/m^*d$, which is exactly what we determined above from the analytical results [see Eq. (6)]. Thus, *the transient character of the ZB oscillations in a collisionless sample is due to the increasing spacial separation of the subpackets* corresponding to the positive and negative energy states. This confirms our previous conclusion that it is not the packet's slow spreading that is responsible for the attenuation (see Discussion). However, as we show below, also spreading may possibly play this role in some cases.

To conclude our analytical discussion of the ZB in bilayer graphene, we consider an interesting property of the velocity squared. If $\hat{v}_x=\partial\hat{H}/\partial\hat{p}_x$ and $\hat{v}_y=\partial\hat{H}/\partial\hat{p}_y$ are calculated directly from the Hamiltonian [Eq. (1)], then it is easy to show that $\hat{v}_x^2=\hbar^2k^2/m^2$ and $\hat{v}_y^2=\hbar^2k^2/m^2$, so that $\hat{v}^2=\hat{v}_x^2+\hat{v}_y^2=2\hbar^2k^2/m^2$ does not depend on time. In the Heisenberg picture, we split the velocity components into "classical" and ZB parts,

$$\hat{v}_x^Z(t)=\frac{\hbar k_y}{mk^2}\begin{pmatrix} k^2\sin(\hbar k^2t/m) & -ik_+^2\cos(\hbar k^2t/m) \\ ik_-^2\cos(\hbar k^2t/m) & -k^2\sin(\hbar k^2t/m)\end{pmatrix},$$

$$\hat{v}_x^c(t)=\frac{\hbar k_x}{mk^2}\begin{pmatrix} 0 & k_+^2 \\ k_-^2 & 0\end{pmatrix}, \tag{22}$$

and similarly for $\hat{v}_y(t)$. Noting that $\{\hat{v}_x^Z(t),\hat{v}_x^c(t)\}=0$, we have $\hat{v}_x(t)^2=\hat{v}_x^Z(t)^2+\hat{v}_x^c(t)^2$. Using Eq. (22), we show that each of these terms is time independent: $\hat{v}_x^Z(t)^2=\hbar^2k_y^2/m^2$ and $\hat{v}_x^c(t)^2=\hbar^2k_x^2/m^2$, and similarly for $\hat{v}_y^Z(t)^2$ and $\hat{v}_y^c(t)^2$. Thus, the velocity squared of the ZB component $\hat{v}^Z(t)^2=\hat{v}_x^Z(t)^2+\hat{v}_y^Z(t)^2=\hbar^2k^2/m^2$ is equal to that of the classical component $\hat{v}^c(t)^2=\hat{v}_x^c(t)^2+\hat{v}_y^c(t)^2=\hbar^2k^2/m^2$.

Finally, in realistic bilayer graphene samples a small gap $E_g$ may appear due to interlayer asymmetry. It was shown for narrow gap semiconductors[3,7] and carbon nanotubes[4] that the Zitterbewegung should also appear in systems with narrow energy gaps (see also Sec. IV below). The main modification, as compared to the situation described above, is that in this case the ZB frequency would be determined by the gap value $\hbar\omega_Z\approx E_g+\hbar^2k_{0y}^2/m^*$. For such an energy spectrum, it is not possible to obtain analytical results.

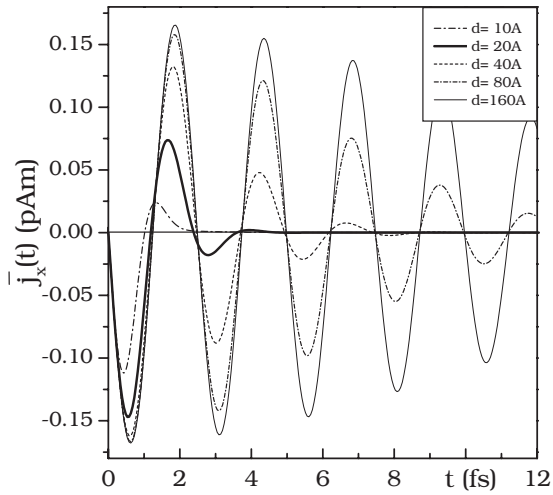


FIG. 2. Oscillatory electric current in the $x$ direction caused by the ZB in monolayer graphene versus time, calculated for a Gaussian wave packet with $k_{0y}=1.2\times10^9$ m$^{-1}$ and various packet widths $d$.

## III. MONOLAYER GRAPHENE

Now, we turn to monolayer graphene. The two-dimensional band Hamiltonian describing its band structure is[19–24]

$$\hat{H}_M=u\begin{pmatrix} 0 & \hat{p}_x-i\hat{p}_y \\ \hat{p}_x+i\hat{p}_y & 0\end{pmatrix}, \tag{23}$$

where $u\approx1\times10^8$ cm/s. The resulting energy dispersion is linear in momentum: $\mathcal{E}=\pm u\hbar k$, where $k=\sqrt{k_x^2+k_y^2}$. The quantum velocity in the Schrödinger picture is $\hat{v}_i=\partial\hat{H}_M/\partial\hat{p}_i$, it does not commute with the Hamiltonian [Eq. (23)]. In the Heisenberg picture, we have $\hat{\boldsymbol{v}}(t)=\exp(i\hat{H}_Mt/\hbar)\boldsymbol{v}\hat{}\times\exp(-i\hat{H}_Mt/\hbar)$. Using Eq. (23), we calculate

$$v_x^{(11)}=u\frac{k_y}{k}\sin(2ukt). \tag{24}$$

The above equation describes the trembling motion with the frequency $\omega_Z=2uk$, determined by the energy difference between the upper and lower energy branches for a given value of $k$. As before, the ZB in the $x$ direction occurs only if there is a nonvanishing momentum $\hbar k_y$. We calculate an average velocity (or current) taken over the wave packet given by Eq. (3). The averaging procedure amounts to a double integral. The latter is not analytical and we compute it numerically. The results for the current $\bar{j}_x=e\bar{v}_x$ are plotted in Fig. 2 for $k_{0y}=1.2\times10^9$ m$^{-1}$ and different realistic packet widths $d$ (see Ref. 25). It is seen that the ZB frequency does not depend on $d$ and is nearly equal to $\omega_Z$ given above for the plane wave. On the other hand, the amplitude of ZB does depend on $d$ and we deal with decay times of the order of femtoseconds. For small $d$, there are almost no oscillations, and for very large $d$, the ZB oscillations are undamped. These conclusions agree with our analytical results for bilayer graphene. The behavior of ZB depends quite critically on the

values of $k_{0y}$ and $d$, which is reminiscent of the damped harmonic oscillator.[26] In the limit $d\to\infty$, our results for the electric current resembles those of Katsnelson[6] for ZB in graphene obtained with the use of the plane wave representation.

## IV. CARBON NANOTUBES

Finally, we consider monolayer graphene sheets rolled into single semiconducting carbon nanotubes (CNT). The band Hamiltonian in this case is similar to Eq. (23) except that, because of the periodic boundary conditions, the momentum $p_x$ is quantized and takes discrete values $\hbar k_x=\hbar k_{n\nu}$, where $k_{n\nu}=(2\pi/L)(n-\nu/3)$, $n=0,\pm1,\ldots$, $\nu=\pm1$, and $L$ is the length of circumference of CNT.[27,28] As a result, the free electron motion can occur only in the $y$ direction, parallel to the tube axis. The geometry of CNT has two important consequences. First, for $\nu=\pm1$, there *always* exists a nonvanishing value of the quantized momentum $\hbar k_{n\nu}$. Second, for each value of $k_{n\nu}$, there exists $k_{-n,-\nu}=-k_{n\nu}$ resulting in the same subband energy $\mathcal{E}=\pm E$, where

$$E=\hbar u\sqrt{k_{n\nu}^2+k_y^2}. \tag{25}$$

The time dependent velocity $\hat{v}_y(t)$ and the displacement $\hat{y}(t)$ can be calculated for the plane electron wave in the usual way and they exhibit the ZB oscillations (see Ref. 4). For small momenta $k_y$, the ZB frequency is $\hbar\omega_Z=E_g$, where $E_g=2\hbar uk_{n\nu}$. The ZB amplitude is $\lambda_Z\approx 1/k_{n\nu}$. However, we are again interested in the displacement $\bar{y}(t)$ of a charge carrier represented by a one-dimensional wave packet analogous to that described in Eq. (3),

$$\psi(y)=\frac{1}{\sqrt{2\pi}}\frac{d^{1/2}}{\pi^{1/4}}\int dk_y e^{-(1/2)d^2k_y^2}e^{ik_yy}\begin{pmatrix}1\\0\end{pmatrix}. \tag{26}$$

The average displacement is $\bar{y}(t)=\bar{y}_Z(t)-\bar{y}_{sh}$, where

$$\bar{y}_Z(t)=\frac{\hbar^2du^2k_{n\nu}}{2\sqrt{\pi}}\int_{-\infty}^{\infty}\frac{dk_y}{E^2}\cos\left(\frac{2Et}{\hbar}\right)e^{-d^2k_y^2}, \tag{27}$$

and $\bar{y}_{sh}=1/2\sqrt{\pi}d\ \mathrm{sgn}(b)[1-\Phi(|b|)]\exp(b^2)$, where $b=k_{n\nu}d$ and $\Phi(x)$ is the error function. The ZB oscillations of $\bar{y}(t)$ are plotted in Fig. 3 for $n=0$, $\nu=\pm1$, and $L=200$ Å. It can be seen that after the transient ZB oscillations disappear, there remains a shift $\bar{y}_{sh}$. Thus, the ZB separates spatially the charge carriers that are degenerate in energy but characterized by $n,\nu$ and $-n,-\nu$ quantum numbers. The current is proportional to $\bar{v}_y=\partial\bar{y}/\partial t$, so that the currents related to $\nu=1$ and $\nu=-1$ cancel each other. To have a nonvanishing current, one needs to break the above symmetry, which can be achieved by applying an external magnetic field parallel to the tube axis.[4]

It can be seen from Fig. 3 that the decay time of ZB in CNT is much larger than that in bilayer and monolayer graphene. The reason is that we considered situation with $k_{0y}=0$, so that the ZB oscillations occur due to "built in" momentum $k_x$ arising from the tube's topology. In other words, the long decay time is due to the one dimensionality of the system. If the circumference of a CNT is increased,

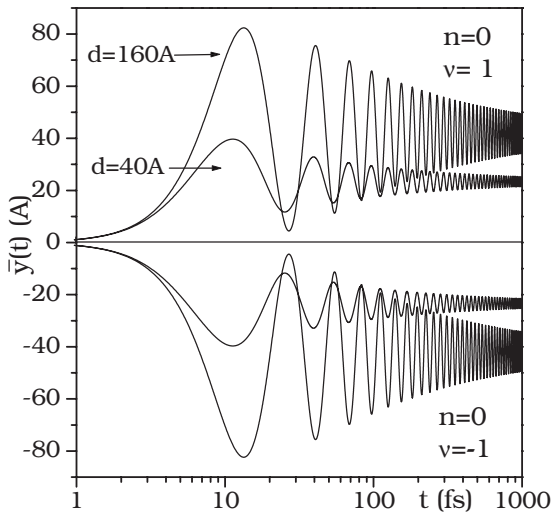


FIG. 3. Zitterbewegung of two charge carriers in the ground subband of a single carbon nanotube of $L=200$ Å versus time (logarithmic scale), calculated for Gaussian wave packets of two different widths $d$ and $k_{0y}=0$. After the ZB disappears, a constant shift remains. The two carriers are described by different quantum numbers $\nu$. At higher times the amplitude of ZB oscillations decays as $t^{-1/2}$ (see text).

the energy gap (and, correspondingly, the ZB frequency) decreases, the amplitude of ZB is larger, but the decay time remains almost unchanged. Our chosen circumference length $L=200$ Å is typical for technologically produced CNTs.

However, it is also possible to prepare a wave packet with an initial nonvanishing momentum $k_{0y}$. Using the method presented above for bilayer graphene [see Eq. (13)], we can decompose the total wave packet [Eq. (26)] into the positive and negative subpackets with the result

$$\psi^p(y,t)=\frac{d^{1/2}}{2^{3/2}\pi^{3/4}}\int dk_y e^{-(1/2)d^2(k_y-k_{0y})^2}e^{ik_yy}e^{-iEt}\begin{pmatrix}1\\k_+/k\end{pmatrix}. \tag{28}$$

The function $\psi^n(y,t)$ is given by a similar expression with the changed signs in front of $E$ and $(k_+/k)$ terms. Here, we use the notation $k=\sqrt{k_{n\nu}^2+k_y^2}$ and $k_+=k_{n\nu}+ik_y$. Now, the oscillating part of $\bar{y}$ is, as before,

$$\int\psi^{n\dagger}y\psi^p dy+\int\psi^{p\dagger}y\psi^n dy=\bar{y}_Z(t,k_{0y}). \tag{29}$$

For $k_{0y}=0$, the above $\bar{y}_Z(t,k_{0y})$ reduces to $\bar{y}_Z(t)$ given by Eq. (27). The average contributions of positive (or negative) terms alone are

$$\int|\psi^p_{(n)}|^2ydy=\frac{1}{2}\bar{y}_c\pm ut\int\frac{k_y|F(k_y)|^2dk_y}{2\sqrt{k_{n\nu}^2+k_y^2}}, \tag{30}$$

where $F(k_y)=d^{1/2}/(2\pi^{1/4})\exp\left[-\frac{1}{2}d^2(k_y-k_{0y})^2\right]$ is the packet function. The sum of the first terms for $\psi^p(y,t)$ and $\psi^n(y,t)$ in Eq. (30) gives $\bar{y}_c$, as before. For $k_{0y}=0$, the second term vanishes which physically means that the relative velocity of the two subpackets is zero, so that they stay together in time.

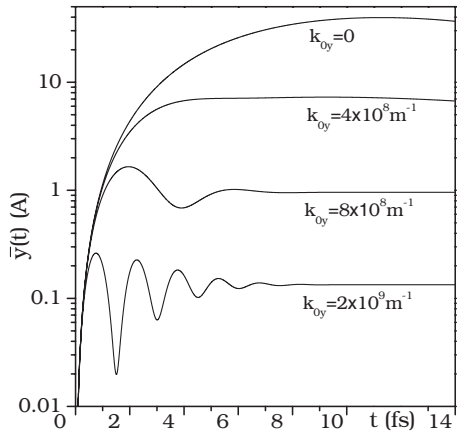


FIG. 4. Zitterbewegung (logarithmic scale) of charge carriers in the ground subband of a single carbon nanotube of $L=200$ Å versus time, calculated for Gaussian wave packet of the width $d=40$ Å and $\nu=+1$. It can be seen that the characteristic decay times are much faster that in Fig. 3, while the oscillation amplitudes are much smaller. The curve for $k_{0y}=0$ is the same as the one for $d=40$ Å and $\nu=+1$ in Fig. 3.

It is for this reason that the decay of ZB is slow (see Fig. 3). If $k_{0y}\neq 0$, the second term in Eq. (30) does not vanish, the two subpackets run away from each other, their overlap diminishes and the ZB disappears much more quickly. This situation is illustrated in Fig. 4. It can be seen that for $k_{0y}\neq 0$, the ZB oscillations disappear on the time scale of a few femtoseconds, as in bilayer and monolayer graphene.

The question remains: what is the physical reason for the slow attenuation of the ZB electron in a collisionless sample shown in Fig. 3, if the subpackets stay together? (As we mentioned in the Introduction, the mathematical expression for the attenuation phenomenon is the Riemann-Lebesgue theorem.) Trying to answer this question we calculated the spreading of the wave subpackets [Eq. (28)] in time. For the initial width $\Delta y\approx 90$ Å, the subpackets reach the width $\Delta y\approx 2600$ Å after the time of 1000 fs. Thus, it is the spreading of the packets that is responsible for the attenuation of ZB. However, it should be noted that while at higher times, the packet's dispersion is linear in time [see Ref. 15 and Fig. 1(d)], the amplitude of ZB oscillations decays as $t^{-1/2}$. A similar slow damping of ZB occurs for one-dimensional relativistic electrons in a vacuum if the average momentum of the subpackets is zero (see Discussion).

## V. DISCUSSION

It is of interest that the ZB phenomena similar to those described above occur also for wave packets representing free relativistic electrons in a vacuum governed by the Dirac equation. This confirms again the strong similarity of the two-band models for nonrelativistic electrons in solids to the description of free relativistic electrons in a vacuum (see Refs. 3, 4, 7, 11, and 12). In contrast to bilayer graphene, the kinematics of the one-dimensional relativistic wave packets may not be described analytically, so the solutions were computed numerically and visualized graphically by Thaller.[29] It was shown that (1) an initial relativistic Gaussian wave packet after spreading is not Gaussian any more. This is analogous to our Eqs. (10) and (11). (2) If an average momentum of the initial positive and negative subpackets is zero, the overlap of the two subpackets remains almost constant in time and the resulting ZB decays quite slowly. This corresponds to our considerations of CNT with $k_{0y}=0$ (see Fig. 3). (It is to be reminded that the two overlapping subpackets are orthogonal to each other.) (3) If the initial average momentum of both subpackets is nonzero, the two subpackets quickly run away from each other and the ZB falls quickly since it is sustained only when the subpackets have some overlap in the position space. This corresponds to our considerations of bilayer graphene (see Fig. 1).

The transient ZB of free relativistic wave packets in a vacuum was also studied numerically by Braun *et al.*[30] It was shown that, for example, the decay times of a typical wave packet having the width $\Delta x=\lambda_c$ and the initial wave vector $k_{0x}=1.37$ a.u. is $2.4\times 10^{-5}$ fs. This should be compared with our predicted decay times of $\Gamma_Z^{-1}=40$ fs for bilayer graphene. It turns out once again that solids are much more promising media for an observation of Zitterbewegung than a vacuum.

The Zitterbewegung phenomenon described above should not be confused with the Bloch oscillations of charge carriers in superlattices, although the latter occur at picosecond frequencies and have comparable picoseconds decay times (see, e.g., Refs. 31–33). However, the Bloch oscillations are basically a one-band phenomenon, they have been realized in superlattices (although this is in principle not the condition *sine qua non*) and, most importantly, they require an external electric field driving electrons all the way to the Brillouin zone boundary. On the other hand, the ZB needs at least two bands and it is a no-field phenomenon. On the other hand, narrow-gap superlattices could provide a suitable medium of its observation. In two very recent papers,[34,35] the authors calculated a static electric conductivity in monolayer graphene using the $2\times 2$ Hamiltonian of Eq. (23). These results are not directly related to our work since we are concerned with the electric currents related to the Zitterbewegung phenomenon at femtosecond frequencies.

In view of our results it is clear that, in order to observe the transient Zitterbewegung, it is necessary to prepare simultaneously a sufficient number of charge carriers in the form of wave packets. If one wants to detect the current, the trembling motion of all carriers must have the same phase. On the other hand, if one wants to see only the remnant displacement, the phase coherence is not necessary. As we said above, the ZB frequency is to a good accuracy given by the corresponding energy difference between the upper and lower energy branches while the amplitude depends strongly on packet's width. For the two graphene materials considered above, one needs an initial momentum in one direction to have the ZB along the transverse direction (see also Ref. 5). For nanotubes, the initial momentum is automatically there due to the circular boundary conditions. As far as the detection is concerned, one needs sensitive current meters or scanning probe microscopy, both working at infrared frequencies and femtosecond to picosecond decay times (see Refs. 36 and 37).

## VI. SUMMARY

In summary, using the two-band structure of bilayer graphene, monolayer graphene, and carbon nanotubes, we show that charge carriers in these materials, localized in the form of Gaussian wave packets, exhibit the transient Zitterbewegung with the decay times of femtoseconds in graphene and picoseconds in nanotubes. Observable dynamical ZB effects, most notably the electric current, are described. It is demonstrated that, after the trembling motion disappears, there remains its "trace" in the form of a persistent charge displacement. It is emphasized that the described ZB in solids is in close analogy to that of the relativistic electron in a vacuum.

## ACKNOWLEDGMENTS

We acknowledge elucidating discussions with I. Birula-Bialynicki. This work was supported in part by the Polish Ministry of Sciences, Grant No. PBZ-MIN-008/P03/2003.

*tomasz.rusin@centertel.pl

[1] E. Schrödinger, Sitzungsber. Preuss. Akad. Wiss., Phys. Math. Kl. **24**, 418 (1930); Schrödinger's derivation is reproduced in A. O. Barut and A. J. Bracken, Phys. Rev. D **23**, 2454 (1981).
[2] F. Cannata, L. Ferrari, and G. Russo, Solid State Commun. **74**, 309 (1990); L. Ferrari and G. Russo, Phys. Rev. B **42**, 7454 (1990).
[3] W. Zawadzki, Phys. Rev. B **72**, 085217 (2005).
[4] W. Zawadzki, Phys. Rev. B **74**, 205439 (2006).
[5] J. Schliemann, D. Loss, and R. M. Westervelt, Phys. Rev. Lett. **94**, 206801 (2005); Phys. Rev. B **73**, 085323 (2006).
[6] M. I. Katsnelson, Eur. Phys. J. B **51**, 157 (2006).
[7] T. M. Rusin and W. Zawadzki, J. Phys.: Condens. Matter **19**, 136219 (2007).
[8] J. Cserti and G. David, Phys. Rev. B **74**, 172305 (2006).
[9] R. Winkler, U. Zulicke, and J. Bolte, Phys. Rev. B **75**, 205314 (2007).
[10] B. Trauzettel, Y. M. Blanter, and A. F. Morpurgo, Phys. Rev. B **75**, 035305 (2007).
[11] W. Zawadzki, in *Optical Properties of Solids*, edited by E. D. Haidemenakis (Gordon and Breach, New York, 1970), p. 179.
[12] W. Zawadzki, in *High Magnetic Fields in the Physics of Semiconductors II*, edited by G. Landwehr and W. Ossau (World Scientific, Singapore, 1997), p. 755.
[13] K. Huang, Am. J. Phys. **20**, 479 (1952).
[14] J. A. Lock, Am. J. Phys. **47**, 797 (1979).
[15] B. M. Garraway and K. A. Suominen, Rep. Prog. Phys. **58**, 365 (1995).
[16] E. McCann and V. I. Fal'ko, Phys. Rev. Lett. **96**, 086805 (2006).
[17] K. S. Novoselov, E. McCann, S. V. Morozov, V. I. Fal'ko, M. I. Katsnelson, U. Zeitler, D. Jiang, F. Schedin, and A. K. Geim, Nat. Mater. **2**, 177 (2006).
[18] M. Novaes and M. A. M. de Aguiar, Phys. Rev. E **70**, 045201(R) (2004).
[19] P. R. Wallace, Phys. Rev. **71**, 622 (1947).
[20] J. C. Slonczewski and P. R. Weiss, Phys. Rev. **109**, 272 (1958).
[21] J. W. McClure, Phys. Rev. **104**, 666 (1956).
[22] K. S. Novoselov, A. K. Geim, S. V. Morozov, D. Jiang, M. I. Katsnelson, I. V. Grigorieva, S. V. Dubonos, and A. A. Firsov, Nature (London) **438**, 197 (2005).
[23] Y. Zhang, Y. W. Tan, H. L. Stormer, and P. Kim, Nature (London) **438**, 201 (2005).
[24] M. L. Sadowski, G. Martinez, M. Potemski, C. Berger, and W. A. de Heer, Phys. Rev. Lett. **97**, 266405 (2006).
[25] J. Schliemann, Phys. Rev. B **75**, 045304 (2007).
[26] L. D. Landau and E. M. Lifshits, *Mechanics* (Fizmatlit, Moscow, 2002).
[27] R. Saito, G. Dresselhaus, and M. S. Dresselhaus, *Physical Properties of Carbon Nanotubes* (Imperial College Press, London, 1999).
[28] H. Ajiki and T. Ando, J. Phys. Soc. Jpn. **62**, 2470 (1993).
[29] B. Thaller, arXiv:quant-ph/0409079 (unpublished).
[30] J. W. Braun, Q. Su, and R. Grobe, Phys. Rev. A **59**, 604 (1999).
[31] R. Martini, G. Klose, H. G. Roskos, H. Kurz, H. T. Grahn, and R. Hey, Phys. Rev. B **54**, R14325 (1996).
[32] V. G. Lyssenko, G. Valusis, F. Loser, T. Hasche, K. Leo, M. M. Dignam, and K. Kohler, Phys. Rev. Lett. **79**, 301 (1997).
[33] Y. A. Kosevich, A. B. Hummel, H. G. Roskos, and K. Kohler, Phys. Rev. Lett. **96**, 137403 (2006).
[34] M. Auslender and M. I. Katsnelson, arXiv:0707.2804 (unpublished).
[35] M. Trushin and J. Schliemann, arXiv:0706.1888 (unpublished).
[36] M. A. Topinka, B. J. LeRoy, S. E. J. Shaw, E. J. Heller, R. M. Westervelt, K. D. Maranowski, and A. C. Gossard, Science **289**, 2323 (2000).
[37] B. J. LeRoy, J. Phys.: Condens. Matter **15**, R1835 (2003).